

# A COMPRESSIVE SAMPLING SCHEME FOR ITERATIVE HYPERSPECTRAL IMAGE RECONSTRUCTION

A. Abrardo, M. Barni, C.M. Carretti, S. Kuiteing Kamdem

E. Magli

Università di Siena  
Dipartimento di Ingegneria dell'Informazione  
{surname}@dii.unisi.it

Politecnico di Torino (Italy)  
Dipartimento di Elettronica  
enrico.magli@polito.it

## ABSTRACT

Compressed Sensing (CS) allows to represent sparse signals through a small number of linear projections. Hence, CS can be thought of as a natural candidate for acquisition of hyperspectral images, as the amount of data acquired by conventional sensors creates significant handling problems on satellites or aircrafts. In this paper we develop an algorithm for CS reconstruction of hyperspectral images. The proposed algorithm employs iterative local image reconstruction based on a hybrid transform/prediction correlation model, coupled with a proper initialization strategy. Experimental results on raw AVIRIS and AIRS images show that the proposed technique yields a very large reduction of mean-squared error with respect to conventional reconstruction methods.

## 1. INTRODUCTION

Compressed sensing (CS) is a relatively new research area that has attracted a lot of interest. CS is concerned with the reconstruction of “compressible” signals from a limited number of linear measurements. That is, if the signal is sparse in some domain, then a limited number of measurements are sufficient to reconstruct the signal exactly with very high probability. Plenty of applications are possible, ranging from image and video to biomedical and spectral imaging, just to mention a few. A single-pixel camera has been demonstrated in [5], which uses a single detector to sequentially acquire random linear measurements of a scene. This kind of design is very interesting for imaging at wavelength outside the visible light, where manufacturing detectors is very expensive. CS could be used to design cheaper sensors, or sensors providing better resolution for an equal number of detectors. E.g., in [8] an architecture is proposed based on Hadamard imaging, coupled with reconstruction techniques borrowed from CS.

How to best reconstruct a spectral image is an open and somewhat elusive problem. The simpler way to proceed is to take separate sets of measurements, e.g. in the spatial or spectral dimensions, and to perform separate reconstructions. However, this “separate” approach does not yield satisfactory performance in terms of mean-squared error (MSE), as the

spatial CS approach completely neglects the spectral correlation, and the spectral approach neglects the spatial one. A more sophisticated approach would entail the use of 3D transforms, so that the whole set of images should be measured and reconstructed at once.

In this paper we take a new look at the reconstruction problem. In [4] it has been shown that 2D spatial CS (i.e., every spectral channel is measured independently) has better performance than spectral CS (in which every spectral vector is measured independently), just because the former approach models correlation in two dimensions, and the latter in only one. However, it should be noted that even spatial CS achieves an MSE that is not small enough for many hyperspectral applications, as the relative error is around  $\pm 5\%$  for sensible values of the number of acquired samples. The key idea is that, in order to improve reconstruction quality, correlation must be exploited in all three dimensions of the spectral cube. To achieve this goal, we propose a new approach, which combines an accurate modeling of the spatial-spectral correlations, with the low complexity of sequential, as opposed to fully joint, band reconstruction. In particular, instead of modeling the correlation by means of a three-dimensional transform, and hence attempting to reconstruct the hyperspectral cube as a whole, we employ a linear correlation model of the hyperspectral image, and iteratively apply this model band by band, improving the quality of the reconstructed image. Since quality of the reconstructed image depends on the initialization of the iterative procedure, we consider different initialization strategies based either on a 2D CS approach or on a simplified 3D strategy [7]. The proposed iterative approach leads to noticeably improve MSE with respect to conventional reconstruction methods.

### 1.1. Compressed Sensing overview

The theory of CS is based on two main principles (see [2]): *sparsity*, and *incoherence*. Sparsity can be defined as the number of non-zero samples (or close to zero samples) and is a property of the signal of interest. A crucial fact is that the best sparsity value for a signal could be in a domain other than the original signal domain. Incoherence pertains to the sens-

ing modality: if the signal is sparse in a certain basis, it has to be spread in the acquisition domain. Random matrices are largely incoherent with any fixed basis, and hence can be used as sensing matrices in virtually any practical applications.

To elaborate, we want to recover an unknown vector  $f \in \mathbb{R}^{N \times 1}$  from a smaller vector  $y \in \mathbb{R}^{M \times 1}$ ,  $M < N$ , of linear measurements:  $y = \Phi f$ , where  $\Phi \in \mathbb{R}^{M \times N}$  is the sensing matrix. We assume that  $f$  is a compressible signal that can be represented as a quasi-sparse vector (i.e. a vector with many null or very small coefficients)  $x \in \mathbb{R}^{N \times 1}$  in a convenient orthonormal basis  $\Psi \in \mathbb{R}^{N \times N}$ , such that  $x = \Psi^T f$ . We assume that the representation  $x$  of  $f$  in the orthonormal basis  $\Psi$  is very concise, i.e. it has few  $K \ll N$  significant elements capturing almost all the energy of  $f$ . Typical sparsity bases include the discrete cosine transform (DCT) and the wavelet transform. A popular recovery approach estimates  $x$  by solving the following linear program:

$$x_{CS} = \arg \min_x \|x\|_{\ell_1} \quad \text{s.t.} \quad \Phi \Psi x = y. \quad (1)$$

This leads to an approximation of  $f$  as  $\hat{f} = \Psi x_{CS}$ . For brevity, we introduce the operator  $LP : (y, \Phi, \Psi) \rightarrow \hat{f}$ , which runs the linear program on a given set of measurements to calculate  $\hat{f}$ . Linear programming is not the only possible recovery strategy, but it does tend to make  $x_{CS}$  sparse. If  $x$  is exactly sparse,  $\Phi$  satisfies the so-called Restricted Isometry Property of suitable order, and  $\Phi$  and  $\Psi$  are incoherent matrices, then an appropriately chosen number  $M < N$  of measurements will yield exact recovery of  $x$  with very high probability. As stated above, it is common to take  $\Phi$  as a random i.i.d. matrix, e.g. a Gaussian matrix, which is incoherent with most  $\Psi$  matrices. If  $x$  is only approximately sparse, the recovery is as good as if one knew ahead of time the locations of the  $K$  largest coefficients of  $x$ .

## 2. PROPOSED RECONSTRUCTION ALGORITHM

### 2.1. Random projections of a hyperspectral image

In the following, we assume that a hyperspectral image is represented as a collection of  $B$  spectral channels, i.e.  $f = [f_0, f_1, \dots, f_{B-1}]$ , where each one-dimensional vector  $f_i$  is the raster-scan ordering of the corresponding two-dimensional spectral channel and has length  $N$ . Corresponding sets of random projections are taken as  $y_i = \Phi_i f_i$ , where  $y_i \in \mathbb{R}^{M \times 1}$ , and  $M < N$ . For simplicity,  $M$  is taken as the same value for all spectral channels. The sensing matrices  $\Phi_i \in \mathbb{R}^{M \times N}$  are taken as Gaussian i.i.d. This setting is amenable to separate spatial reconstruction of each spectral channel using a two-dimensional transform as sparsity domain. However, we expect that separate spatial reconstruction does not yield a sufficiently accurate estimate of the original image, since it lacks modeling of spectral correlation, which is very strong for hyperspectral images.

The proposed algorithm performs iterative sequential band reconstruction, employing linear prediction, as opposed to transform band approaches, to model spectral correlation.

### 2.2. Prediction

In the following we describe the linear prediction stage employed during reconstruction. The predictor operates in a blockwise fashion. Prediction of spectral channel  $i$  is performed dividing the channel into non-overlapping spatial blocks of size  $16 \times 16$  pixels. Each block is predicted from the spatially co-located block in a reference spectral channel  $l$  (typically the previous or next band). Focusing on a single  $16 \times 16$  block, we denote by  $f_{m,n,i}$  the pixel of an hyperspectral image in  $m$ -th line,  $n$ -th pixel, and  $i$ -th band, with  $m, n = 0, \dots, 15$ , and  $i = 0, \dots, B - 1$ .

Samples  $f_{m,n,i}$  belonging to the block are predicted from the samples  $\hat{f}_{m,n,l}$  of the *reconstructed* reference band. In particular, a least-squares estimator [6] is computed over the block. First, a gain factor is calculated as  $\alpha = \frac{\alpha_N}{\alpha_D}$ , with  $\alpha_N = \sum_{m,n} [(\hat{f}_{m,n,l} - \mu_l)(\hat{f}_{m,n,i} - \mu_i)]$  and  $\alpha_D = \sum_{m,n} [(\hat{f}_{m,n,l} - \mu_l)^2]$ .  $\mu_i$  and  $\mu_l$  are the average values of the co-located reconstructed blocks in bands  $f_i$  and  $f_l$ . Then the predicted values within the block are computed for all  $m, n = 0, \dots, 15$  as  $\tilde{f}_{m,n,i}^{(l)} = \mu_i + \alpha(\hat{f}_{m,n,l} - \mu_l)$ .

This one-step predictor is employed in such a way as to take full advantage of the correlation between bands. In particular, the current band is very correlated with its two adjacent bands, while the correlation tends to decrease moving further away. Eventually, we define a predictor for a block in the current band  $f_i$  as the average of two predictors obtained from the previous and the next band [1].  $\tilde{f}_{m,n,i} = (\tilde{f}_{m,n,i}^{(i-1)} + \tilde{f}_{m,n,i}^{(i+1)})/2$ . For brevity, we define an operator  $\Pi(\hat{f}_{i-1}, \hat{f}_{i+1}) = p_i$  that applies this predictor to the two adjacent reconstructed spectral channels  $f_{i-1}$  and  $f_{i+1}$  in a blockwise manner as described above, yielding a predicted spectral channel  $p_i$ . Exceptions are made for the first and last band, where only the available previous/next band is used for the prediction.

### 2.3. Iterative CS reconstruction

The idea behind the iterative reconstruction is that, if we can obtain a prediction of a spectral channel  $f_i$ , e.g. applying the operator  $\Pi$  to channels  $f_{i-1}$  and  $f_{i+1}$  of some initial reconstruction, then we can cancel out the contribution of this predictor from the measurements of  $f_i$ , and reconstruct only the prediction error instead of the full spectral channel. If the predictor is accurate, the prediction error is expected to be more sparse than the full signal, and the reconstruction will yield better results. In particular, the iterative procedure starts from the initial reconstruction  $\hat{f}$  of all spectral channels. At this stage, we do not specify how we generate such initial re-

---

**Algorithm 1** Iterative reconstruction algorithm

---

**INPUT:** measurements  $y_i$  and matrices  $\Phi_i$ , with  $i = 0, \dots, B - 1$ ; 2D DCT matrix  $\Psi$ ; number of iterations  $W$ .

**OUTPUT:** reconstructed channels  $\hat{f}_i$ , with  $i = 0, \dots, B - 1$

$$\hat{f} = F(y, \Phi)$$

*Iterative reconstruction*

$j = 0$

**while**  $j < W$  **do**

$j \leftarrow j + 1$

**for**  $i = 0$  **to**  $B - 1$  **do**

$p_i \leftarrow \Pi(\hat{f}_{i-1}, \hat{f}_{i+1})$

$\epsilon_i \leftarrow y_i - \Phi_i p_i$

$\hat{f}_i \leftarrow p_i + \text{LP}(\epsilon_i, \Phi_i, \Psi)$

**end for**

**end while**

---

construction, which is generically denoted by  $\hat{f} = F(y, \Phi)$  to indicate that it is computed from random projections  $y$  and measurement matrixes  $\Phi$ . Then, for every channel  $f_i$ , we first obtain  $p_i = \Pi(\hat{f}_{i-1}, \hat{f}_{i+1})$ . After that, we compute prediction error measurements as  $\epsilon_i = y_i - \Phi_i p_i$ , and we use  $\epsilon_i$  to reconstruct  $\hat{f}_i = p_i + \text{LP}(\epsilon_i, \Phi_i, \Psi)$ . This process is performed on all bands, and is iterated until convergence. Note that, since the operator LP is convex, and the predictor is linear, this algorithm can be cast in terms of projections onto convex sets [3], guaranteeing convergence to the intersection of the constraint sets (if not empty). The proposed iterative reconstruction scheme is shown in Algorithm 1.

#### 2.4. Preliminary experimental analysis with initial separate 2D reconstruction

We have carried out some experiments to preliminarily assess the validity of the proposed algorithm when the initial reconstruction images  $\hat{f}_i$  are computed with the operator LP using separate 2D DCT transforms band by band, i.e.,  $\hat{f}_i \leftarrow \text{LP}(y_i, \Phi_i, \Psi)$ . In particular, Figure 1 shows the MSE behavior experienced on AVIRIS images<sup>1</sup> as a function of the number of iterations  $W$  for different values of the number of projections  $M$ . A similar behavior is observed for AIRS images. Note that for medium to high  $M$ , iterations are effective in reducing MSE, e.g., for  $M > 400$  the proposed algorithm improves the MSE up to a factor of 35 with respect to the initial reconstruction. Moreover, convergence to the minimum attainable MSE is obtained in a relatively small number of iterations. For lower  $M$ , convergence is slower and MSE reduction is less effective. In particular, for very low  $M$ , e.g. for  $M = 100$  convergence is very slow and MSE reduction is negligible. In essence, the algorithm shows a threshold behavior with respect to the initial reconstructed images  $\hat{f}_i$ : a poor

<sup>1</sup>A detailed description of AVIRIS test images is given in Section 3.

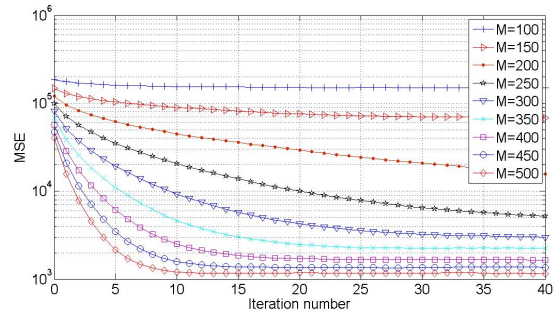


**Fig. 1.** MSE behavior on AVIRIS images of Algorithm 1 as a function of the number of iterations  $W$  with initial separate 2D reconstruction.

initial reconstruction prevents the iterative algorithm to improve the MSE while if the initial reconstruction's MSE falls below a minimum threshold, the improvement is remarkable and convergence very fast.

#### 2.5. Improving initial reconstruction by means of Kronecker CS

Given the above, we have investigated the possibility of implementing a more sophisticated reconstruction algorithm which allows the proposed scheme to achieve good performance even for low  $M$ , i.e., for high compression ratios. To this aim, we considered the simplified 3D reconstruction scheme proposed in [7], where it is shown that Kronecker product matrices are a natural way to generate sparsifying and measurement matrices for the application of CS to multi-dimensional signals, resulting in a formulation that is denoted by Kronecker Compressive Sensing (KCS). In KCS, starting from the assumption that the signal structure along each dimension can be expressed via sparsity, Kronecker product sparsity bases combine the structures for each signal dimension into a single matrix and representation. This allows to obtain separable transforms matrices, thus maintaining the computational complexity to an acceptable level. Similarly, Kronecker random product measurement matrices for multi-dimensional signals can be implemented by performing a sequence of separate random measurements obtained along each dimension. Given the above, the application of KCS to the problem at hand is straightforward: the separate (band by band) random projections  $y_i = \Phi_i f_i$  can be used to get a reconstruction scheme which profitably exploits correlation in all dimensions by using a separable 3D Kronecker product sparsity domain. More specifically, we consider DCT transforms for both spatial and spectral domains since DCT transform is better than other typical transforms used in CS (e.g. Wavelet transform) on small spatial crops, while a wavelet transform would arguably provide better performance over a larger image. Accordingly, denoting by  $\Psi^2$  and  $\Psi^1$  the DCT sparsifying operator for the spatial and spectral domain, respectively, reconstruction may be obtained by means of

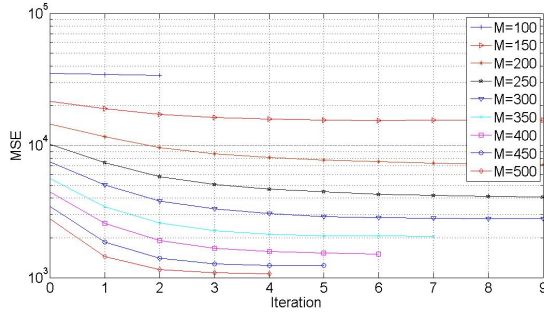


**Fig. 2.** MSE behavior on AVIRIS images of Algorithm 1 with 3D Kronecker starting point, as a function of the number of iterations  $W$ .

linear program reconstruction  $LP_{3D} : (y, \Phi, \Psi^2 \otimes \Psi^1) \rightarrow \hat{f}$ , where  $y = [y_0, y_1, \dots, y_{B-1}]$ ,  $\Phi = [\Phi_0, \Phi_1, \dots, \Phi_{B-1}]$  and  $\Psi^2 \otimes \Psi^1$  is the Kronecker product between  $\Psi^2$  and  $\Psi^1$ . The reconstructed set of images  $\hat{f}$  can then be used as starting point for the iterative algorithm proposed in Algorithm 1. To assess the effectiveness of such an approach, in Figure 2 we show the MSE behavior experienced on AVIRIS images as a function of  $W$ , for different  $M$ , when the starting point of the iterative scheme proposed in Algorithm 1 is obtained through Kronecker 3D reconstruction. Comparing with Figure 1 it can be observed that, as expected, the MSE starting point is much lower and convergence is achieved in few iterations. Moreover, despite 3D Kronecker reconstruction already exploits correlation in the spectral domain, the proposed iterative algorithm still allows to improve the MSE up to a factor of 3 with respect to the initial reconstruction. In the next section, we describe in more details the experiments we conducted to evaluate the performance of the two proposed reconstruction schemes, namely iterative compressed sampling (ICS) and Kronecker-iterative compressed sampling (KICS), which are both based on the iterative procedure described in Algorithm 1, with the initial point computed by means of LP and  $LP_{3D}$ , respectively.

### 3. RESULTS

We report reconstruction results on a few scenes that are used as reference for onboard lossy compression in the “multispectral and hyperspectral data compression” working group of the Consultative Committee for Space Data Systems (CCSDS), namely scene *sc0* of AVIRIS (Yellowstone) and granule 9 (*gran9*) of AIRS. AVIRIS is a spectrometer with 224 bands, and the size of this image is 512 lines and 680 pixels. AIRS is an ultraspectral sounder with 2378 spectral channels, used to create 3D maps of air and surface temperature. In the CCSDS dataset, only 1501 bands are considered; the unstable channels have been removed as they have little

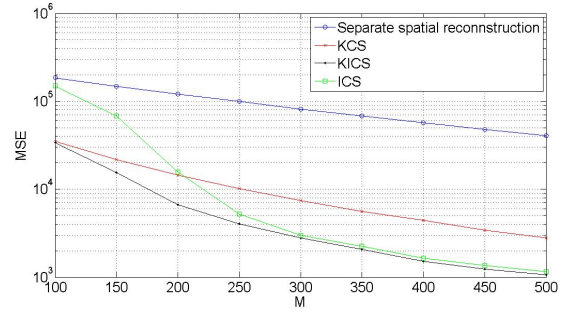


**Fig. 3.** Reconstruction of AVIRIS scene: MSE versus  $M$  for different reconstruction schemes.

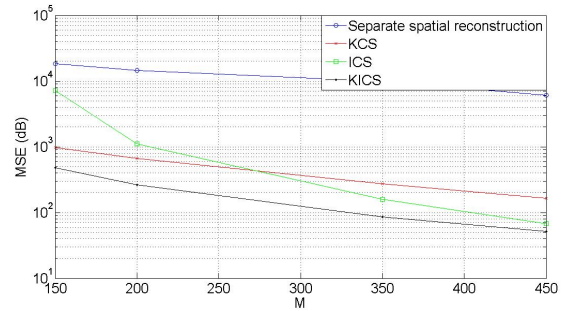


**Fig. 4.** Reconstruction of AIRS scene: MSE versus  $M$  for different reconstruction schemes.

or no scientific interest. The spatial size is 90 pixels and 135 lines. Because of the complexity of the reconstruction process and the large amount of data, we do not use the complete images, but rather a  $32 \times 32$  spatial crop with all spectral channels. Both are *raw* images, i.e. they are the output of the detector, with no processing, calibration or denoising applied. These images are noisier than the corresponding processed images, but more realistic for application to onboard sensors.

We compare results of the proposed ICS and KICS with those obtained through separate spatial reconstruction (S2D) of each spectral channel and through 3D KCS. The reconstruction algorithm for the iterative schemes is run for 40 iterations, with several values of  $M$ . Results in terms of MSE versus  $M$  are shown in Figures 3 and 4 for the AVIRIS and AIRS scenes, respectively. As can be seen, S2D spatial reconstruction yields very large mean-squared error (MSE), typically in excess of  $5 \cdot 10^4$  for AVIRIS and of  $7 \cdot 10^3$  for AIRS. Considering that the average signal energy for this crop is equal to  $2.76 \cdot 10^7$  for AVIRIS and  $4.85 \cdot 10^6$  for AIRS, spatial reconstruction yields an average percentage error of nearly  $\pm 4\%$  both test images, which is inadequate for most applications. As anticipated in Figure 1, the proposed ICS reconstruction algorithm allows to improve the MSE up to a factor of 35 for high  $M$ , but it is not effective for low  $M$ .

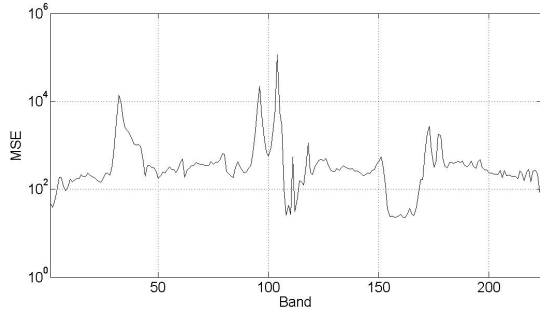


**Fig. 5.** Reconstruction of AVIRIS scene: MSE for each band, with  $M = 450$ .

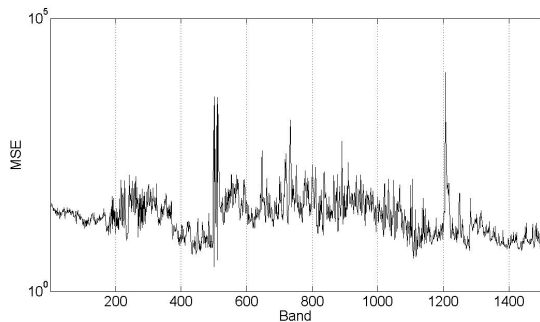


**Fig. 6.** Reconstruction of AIRS scene: MSE for each band, with  $M = 450$ .

On the other hand, the 3D KCS reconstruction without iterative predictions performs quite well for low  $M$  but its performance are not so good for high  $M$ , e.g., it is even worse than ICS for  $M > 200 - 250$ . Eventually, KICS gives the best performance over the whole range of considered  $M$ . In other words, combining 3D KCS with predictive CS allows to accurately reconstruct original images requiring a number of linear measurements much smaller than the original samples. On the other hand, average results provide a somewhat biased picture though. In Fig. 5 and 6, the individual MSE per band and for  $M = 450$  obtained through KICS algorithm on AVIRIS and AIRS scene is shown, respectively. As can be seen, in most bands the MSE is very small, between 100 and 400. The average MSE is biased by a relatively small number of bands which are reconstructed with large error. Visual inspection shows that e.g. band 104 is extremely noisy (hence not at all sparse) and contains almost no information, while band 32 is misregistered with respect to band 31, yielding poor prediction. This shows that, on average, a much lower relative error can be achieved in most bands, except for noisy bands, which are not very important altogether, or misregistered bands, where improved prediction models can be employed to improve the reconstruction.

#### 4. CONCLUSION AND FUTURE WORK

We have proposed an iterative reconstruction algorithm that improves over both spatially separate and 3D Kronecker reconstructions of hyperspectral images from their random projections, able to noticeably decrease the MSE for both AVIRIS and AIRS images. These are raw images, and since the relative errors achieved by the proposed algorithm are typically below 1% for  $M = 350$  or larger, we conclude that CS can accurately reconstruct these images requiring a number of linear measurements not larger than one third of the original samples, and usually less in most bands. We believe that this figure can be reduced even more, and this will be subject of future research. The algorithm can be improved in several ways, potentially reducing the number of required measurements. E.g., taking larger spatial crops will allow to employ a wavelet transform, which provides a better sparsity model. The prediction can be made adaptive, avoiding to use very noisy or misregistered images as predictors.

#### 5. REFERENCES

- [1] A. Abrardo, M. Barni, and E. Magli. Low-complexity predictive lossy compression of hyperspectral and ultra-spectral images. In *ICASSP2011 (May 22-27)*, 2011.
- [2] E. Candes and M. Wakin. An introduction to compressive sampling. *IEEE Signal Processing Magazine*, 25(2):21–30, 2008.
- [3] P. Combettes. The foundations of set theoretic estimation. *Proceedings of the IEEE*, 81:182–208, 1993.
- [4] M. Duarte and R. Baraniuk. Kronecker product matrices for compressive sensing. In *Proc. of IEEE ICASSP*, 2010.
- [5] M. Duarte, M. Davenport, D. Takhar, J. Laska, T. Sun, K. Kelly, and R. Baraniuk. Single-pixel imaging via compressive sampling. *IEEE Signal Processing Magazine*, 83:83–91, Mar 2008.
- [6] M. Slyz and L. Zhang. A block-based inter-band lossless hyperspectral image compressor. In *Data Compression Conference, 2005. Proceedings. DCC 2005*, pages 427–436. IEEE, 2005.
- [7] M. Trocan, T. Maugey, E. Tramel, J. Fowler, and B. Pesquet-Popescu. Multistage compressed-sensing reconstruction of multiview images. In *Multimedia Signal Processing (MMSP), 2010 IEEE International Workshop on*, pages 111–115, oct. 2010.
- [8] R. Willett, M. Gehm, and D. Brady. Multiscale reconstruction for computational spectral imaging. In *Proc. of SPIE Electronic Imaging*, 2007.